

## Supporting information

### Vibrational dynamics (IR, Raman, NRVS) and DFT study of new antitumor tetranuclear stannoxane cluster, Sn(IV)-oxo-{di-*o*-vanillin} dimethyl dichloride

Farukh Arjmand,<sup>a,\*</sup> Surbhi Sharma,<sup>a</sup> Mohammad Usman,<sup>a</sup> Bogdan M. Leu,<sup>b,\*</sup> Michael Y. Hu,<sup>b</sup> Loic Toupet,<sup>c</sup> David Gosztola,<sup>d</sup> and Sartaj Tabassum<sup>a</sup>

<b>S No.</b>	<b>Table of contents</b>	<b>Page No.</b>
1	<b>Materials and instrumentation</b>	S2
2	<b>Computational methodology</b>	S2
3	<b>NRVS experimental</b>	S3
4	<b>Raman experimental</b>	S3
5.	<b>DNA binding experimental</b>	S3
6.	<b>Docking experimental</b>	S4
7	<b>Synthesis of 1</b>	S4
8	<b>Description of X-ray Crystal structure</b>	S5
	<b>Table for and stucture refinement data for crystal</b>	S6
	<b>Tables for selected bond lengths and angle of 1</b>	S7, S8
9	<b>Table for Mode Composition Factors, calculated frequency and Mode Description of various types of vibrations in 1</b>	S8-S10
10	<b>Far-IR spectrum of 1</b>	S10
11	<b>ESI Mass spectrum of 1</b>	S11
12	<b>UV-vis and emission spectra of [CT-DNA-1] system</b>	S11, S12
13	<b><i>In vitro</i> antitumor activity</b>	S12
14	<b>Growth curve showing % control vs. drug or complex concentration (µg/ml)</b>	S13, S14
15	<b>DFT/B3LYP optimized structure of complex 1</b>	S15
16	<b>Tables for DFT/B3LYP calculated bond lengths and angle of 1 in comparison to the X-ray data</b>	S15, S16
17	<b>DFT-optimized structure coordinates of complex 1</b>	S17, S18
18	<b>References</b>	S18, S19

## **Experimental**

### **Materials and instrumentation**

*o*-vanillin, dimethyltin(IV) dichloride and triethylamine were purchased from Sigma Aldrich. All reagents were of the best commercial grade and were used without further purification. Elemental analysis was carried out on Carlo Erba Analyser Model 1106. Molar conductance was measured at room temperature on Eutech con 510 electronic conductivity bridge. Fourier-transform infrared (FTIR) spectra were recorded on an Interspec 2020 and Spectrum Two (Perkin Elmer) FTIR spectrometers. ESI-MS spectra were recorded on Micromass Quattro II triple quadrupole mass spectrometer. NMR spectra were obtained on a Bruker DRX-400 spectrometer with Me<sub>2</sub>SO-*d*<sub>6</sub> as solvent. Electronic spectra were recorded on UV-1700 PharmaSpec UV-vis spectrophotometer (Shimadzu) in DMSO using cuvettes of 1 cm path length and data were reported in  $\lambda_{\text{max}}/\text{nm}$ .

### **Computational methodology**

All computations reported within were performed using ORCA computational package.<sup>1</sup> Initial coordinates were taken from single crystal X-ray data and used for gas-phase ground state optimization. Gas-phase harmonic vibrational frequencies and IR intensities were calculated based on optimized geometry. The ground state geometry optimization and frequency analyses of the **1** was performed at the hybrid functional B3LYP level of DFT adding def2-TZVP basis set for Sn atom and def2-SVP basis set for all other atoms.<sup>2</sup> To accelerate the computation, we utilized the resolution of identity (RI) approximation with the decontracted auxiliary def2-TZV/J or def2-SVP/J Coulomb fitting basis sets and the chain-of-spheres (RIJCOSX) approximation to exact exchange as implemented in ORCA.<sup>3</sup>

The mode composition factor, representing the fraction of the total vibrational kinetic energy of each mode associated with the motion of a Sn atom, is calculated according to:<sup>4</sup>

$$\frac{(mr^2)_{Sn}}{\sum mr^2 \text{ all atoms}} = e_{Sn}^2 \quad (S1)$$

Where  $m$  and  $r$  are the atomic mass and atomic displacements, respectively (gray bars in Fig. 3).

For each predicted mode we generated a Lorentzian function with the area equal to  $e_{Sn}^2$  and a full-width-at-half-maximum of  $10 \text{ cm}^{-1}$ . The sum of these functions, for all four Sn atoms, is shown as a red line in Fig. 3.

The NRVS experiment was carried out at beamline 30-ID of the Advanced Photon Source, Argonne National Laboratory<sup>5</sup> at a temperature of 165 K, with an incident X-ray beam of 23.88 keV, and an energy resolution of 1.3 meV, measured by nuclear forward scattering on  $^{119}\text{Sn}$ -enriched tin oxides.<sup>5</sup> Multiple scans were added to obtain the excitation probability, from which the partial vibrational density of states was extracted using the program PHOENIX.<sup>6</sup>

The Raman experiment was performed at the Center for Nanoscale Materials, Argonne National Laboratory at room temperature using 633-nm excitation from a helium-neon laser with 1-mW incident power and a Raman microscope (inVia Reflex, Renishaw, Inc.). Scattered light was collected through a 50X objective (Leica, NA = 0.75). The spectra are the result of averaging 100 20-second integrations.

CT-DNA binding experiments were performed in Tris-HCl/NaCl (5:50 mM) buffer at pH 7.2 which included absorption spectral traces, and emission spectroscopy conformed to the standard methods and practices previously adopted by our laboratory.<sup>7-9</sup> While measuring the absorption spectra an equal amount of CT-DNA was added to both the compound solution and the reference solution to eliminate the absorbance of the CT-DNA itself, and absorbance of the Tris buffer was subtracted through base line correction.

HEX 8.0 software was used for Molecular docking studies,<sup>10</sup> which is an interactive molecular graphics program for calculating and displaying feasible docking modes of an enzymes and DNA molecule. Structure of the **1** was converted it into PDB format from mol format while the PDB file of the B-DNA dodecamer d(CGCGAATTCGCG)<sub>2</sub> (PDB ID: 1BNA), was downloaded from the protein data bank (<http://www.rcsb.org/pdb>). Visualization of the docked pose has been done by using CHIMERA ([www.cgl.ucsf.edu/chimera](http://www.cgl.ucsf.edu/chimera)), PyMol (<http://pymol.sourceforge.net/>) and Discovery Studio molecular graphics program.

### **Synthesis of tetranuclear Sn(IV)-oxo-{di-*o*-vanillin}dimethyl dichloride**

A methanolic solution of dimethyltin(IV) dichloride (0.219 g, 1 mmol) was added drop wise to the solution of *o*-vanillin (0.152 g, 1 mmol) in the methanol in presence of triethylamine. The resulting mixture was refluxed for about 10 h until a yellow solid was precipitated which was filtered, washed with hexane yielding 67% of crude product. Suitable yellow crystals for single X-ray diffraction were obtained by recrystallizing the product in MeOH/DCM (1:4) mixture.

Yield: (67%); M.p. 197 °C; Anal. Calc. for C<sub>24</sub>H<sub>38</sub>Sn<sub>4</sub>Cl<sub>2</sub>O<sub>8</sub> (%): Calc. C, 28.82; H, 3.83. Found: C, 28.67; H, 3.89. FTIR (KBr pellet,  $\nu_{\max}/\text{cm}^{-1}$ ): 2918  $\nu(\text{C-H})$ , 1633  $\nu(\text{C=O})$ , 1026  $\nu(\text{OCH}_3)$ , 1469–446,  $\nu(\text{aromatic C=C})$ , 1244–1299  $\nu(\text{phenolic C-O})$ , 522 and 566  $\nu(\text{Sn-C})$ , 585  $\nu(\text{Sn-O})$ , 186, 114  $\nu(\text{Sn-O-Sn})$ .

UV-vis ( $1 \times 10^{-3}$  M, DMSO,  $\lambda_{\max}$  nm): 265 and 341. <sup>1</sup>H NMR (400 MHz, DMSO-*d*<sub>6</sub>, ppm): 1.18–1.00 (s, 24H, Sn-CH<sub>3</sub>), 3.83 (s, 3H, -OCH<sub>3</sub>, vanillin), 6.91–7.39 (m, 6H, aromatic), 9.41 (s, 1H, aromatic CHO). <sup>119</sup>Sn-NMR (149.19 MHz, DMSO-*d*<sub>6</sub>, ppm): -134, -258 and -389. ESI-MS (DMSO) (*m/z*): 522 [C<sub>11</sub>H<sub>16</sub>Sn<sub>2</sub>Cl<sub>2</sub>O<sub>3</sub>]<sup>+</sup>, 151 [C<sub>8</sub>H<sub>7</sub>O<sub>3</sub>]<sup>+</sup>. CCDC: 1403573.

### **Description of X-ray Crystal structure**

Single crystals suitable for X-ray study of the **1** were obtained after slow evaporation of the reaction mixture at room temperature. Single crystal X-ray structural studies of complex was performed on a CCD Oxford Diffraction X caliber Saphir 3 diffractometer employing graphite-monochromated Mo-K $\alpha$  radiation generated from a fine-focus sealed tube ( $\lambda = 0.71073\text{\AA}$ ) at 140(2) K. Data collection strategy was evaluated by using the Crys Alis Pro CCD software. Collections of data were observed by the standard  $\omega$  scan techniques and were scaled and reduced using Crys Alis Pro RED software. The structure was solved by direct methods using SIR-97<sup>11</sup> and refined by least-squares methods on  $F^2$  using SHELXL-97.<sup>12</sup> The positions of all atoms were obtained by direct methods. Anisotropic thermal parameter were assigned to all non-hydrogen atoms and the remaining hydrogen atoms were placed in geometrically constrained position and refined as riding atoms with a common fixed isotropic thermal parameter. The drawing of the complex was realized with PLATON.<sup>13</sup>

**Table S1** Crystal and structure refinement data for **1**.

CCDC	1403573
formula	C <sub>24</sub> H <sub>38</sub> Sn <sub>4</sub> Cl <sub>2</sub> O <sub>8</sub>
Fw (g mol <sup>-1</sup> )	1000.28
crystal system	Monoclinic
space group	P 21/m
a (Å)	7.5613(2)
b (Å)	18.8087(3)
c (Å)	11.8932(2)
α (deg)	90
β(deg)	104.691(2)
γ (deg)	90
U (Å <sup>3</sup> )	1636.13 (6)
Z	4
ρ <sub>calc</sub> (g/cm <sup>3</sup> )	2.030
μ (mm <sup>-1</sup> )	25.853
F(000)	960.0
crystal size (mm)	0.284 x 0.215 x 0.114
Temp (K)	150 K
measured reflns	16206
unique reflns	3236
θ Range (deg)/ completeness (%)	3.842 to 70.652 deg
GOF <sup>a</sup>	1.050
R <sup>b</sup> [I>2σ(I)]	0.0600
wR <sub>2</sub> <sup>b</sup> (all data)	0.1557
largest diff. peak/hole (e.Å <sup>-3</sup> )	2.028/-2.450

<sup>a</sup>Gof is defined as  $\{\sum[w(F_o^2-F_c^2)]/(n-P)\}^{1/2}$  where  $n$  is the number of data and  $p$  is the number of parameters. <sup>b</sup>R =  $\{\sum||F_o|-|F_c||/\sum|F_o|\}$ ,  $wR^2 = \{\sum w(F_o^2-F_c^2)^2 / \sum w(F_o^2)^2\}^{1/2}$ .

**Table S2** Selected bond lengths (Å) of **1**.

<b>Bond lengths</b>	<b>(Å)</b>
Sn(1)-O(4)	2.013(3)
Sn(1)-C(4)	2.102(5)
Sn(1)-C(3)	2.107(5)
Sn(1)-O(5)	2.140(3)
Sn(1)-O(3)	2.468(4)
Sn(2)-O(4)	2.061(5)
Sn(2)-C(6)	2.097(7)
Sn(2)-C(5)	2.096(7)
Sn(2)-O(3)#1	2.383(3)
Sn(2)-O(3)	2.383(3)
Sn(2)-O(1)	2.460(4)
Sn(2)-O(1)#1	2.460(4)
Sn(3)-O(5)	1.976(5)
Sn(3)-C(2)	2.116(8)
Sn(3)-C(1)	2.119(8)
Sn(3)-Cl(1)	2.6052(15)
Sn(3)-Cl(1)#1	2.6052(15)

**Table S3** Selected bond angles of **1**

<b>Bond Angle</b>	<b>[deg]</b>
O(4)-Sn(1)-O(5)	74.16(17)
O(4)-Sn(1)-O(3)	68.90(14)
O(5)-Sn(1)-O(3)	142.89(14)
O(4)-Sn(2)-O(3)#1	69.98(9)
O(4)-Sn(2)-O(3)	69.98(9)
O(3)#1-Sn(2)-O(3)	139.71(18)
O(4)-Sn(2)-O(1)	143.76(9)
O(3)#1-Sn(2)-O(1)	146.24(13)
O(3)-Sn(2)-O(1)	73.98(13)
O(4)-Sn(2)-O(1)#1	143.76(9)
O(3)#1-Sn(2)-O(1)#1	73.97(13)
O(3)-Sn(2)-O(1)#1	146.24(13)
O(1)-Sn(2)-O(1)#1	72.29(18)
O(5)-Sn(3)-Cl(1)	83.48(3)
O(5)-Sn(3)-Cl(1)#1	83.48(3)
C(2)-Sn(3)-Cl(1)#1	92.50(5)

C(1)-Sn(3)-Cl(1)#1	92.62(4)
Cl(1)-Sn(3)-Cl(1)#1	166.96(7)
Sn(2)-O(3)-Sn(1)	96.13(13)
Sn(1)-O(4)-Sn(1)#1	110.4(2)
Sn(1)-O(4)-Sn(2)	124.72(12)
Sn(1)#1-O(4)-Sn(2)	124.72(12)
Sn(3)-O(5)-Sn(1)#1	128.89(11)
Sn(3)-O(5)-Sn(1)	128.89(11)
Sn(1)#1-O(5)-Sn(1)	101.1(2)
Sn(3)-C(1)-H(1A)	109.5
Sn(3)-C(1)-H(1B)	109.5
Sn(3)-C(1)-H(1C)	109.5

**Table S4** Mode composition factors, calculated frequency and mode description of various types of vibrations in **1**.

Type of vibration	Bonds involved	Calculated frequency (cm <sup>-1</sup> )	$e_{Sn(1)}^2$	$e_{Sn(2)}^2$	$e_{Sn(3)}^2$	$e_{Sn(4)}^2$	$\sum_{i=1}^4 e_{Sn(i)}^2$	Mode description
Doming	All (O-Sn-O)	37, 108, 119, 129, 153, 154	0-0.03	0-0.03	0-0.03	0-0.05	0.05-0.07	Perpendicular to the plane
Out-of-plane	O <sub>1</sub> -Sn <sub>2</sub> -O <sub>6</sub>	47	0.00	0.02	0.01	0.00	0.03	Wagging
	O <sub>1</sub> -Sn <sub>2</sub> -O <sub>6</sub> O <sub>1</sub> -Sn <sub>2</sub> -O <sub>3</sub> O <sub>6</sub> -Sn <sub>2</sub> -O <sub>8</sub> O <sub>3</sub> -Sn <sub>1</sub> -O <sub>2</sub> Sn <sub>2</sub> -O <sub>3</sub> -Sn <sub>1</sub> Sn <sub>2</sub> -O <sub>4</sub> -Sn <sub>1</sub>	51	0.00	0.01	0.00	0.00	0.02	Twisting Wagging Wagging Wagging Wagging Wagging
	O <sub>1</sub> -Sn <sub>2</sub> -O <sub>6</sub> O <sub>6</sub> -Sn <sub>2</sub> -O <sub>8</sub>	59	0.00	0.01	0.01	0.01	0.03	Twisting Twisting
	O <sub>1</sub> -Sn <sub>2</sub> -O <sub>6</sub> O <sub>6</sub> -Sn <sub>2</sub> -O <sub>8</sub> O <sub>3</sub> -Sn <sub>2</sub> -O <sub>1</sub>	166	0.01	0.00	0.02	0.00	0.03	Twisting
	O <sub>3</sub> -Sn <sub>2</sub> -O <sub>1</sub> O <sub>1</sub> -Sn <sub>2</sub> -O <sub>6</sub> O <sub>6</sub> -Sn <sub>2</sub> -O <sub>8</sub> O <sub>3</sub> -Sn <sub>1</sub> -O <sub>2</sub>	175	0.00	0.02	0.02	0.00	0.05	Twisting Twisting Twisting Twisting
	O <sub>3</sub> -Sn <sub>2</sub> -O <sub>1</sub>	192	0.02	0.01	0.00	0.01	0.07	Wagging

	O <sub>1</sub> -Sn <sub>2</sub> -O <sub>6</sub> O <sub>6</sub> -Sn <sub>2</sub> -O <sub>8</sub> O <sub>3</sub> -Sn <sub>1</sub> -O <sub>2</sub>							
	O <sub>7</sub> -Sn <sub>4</sub> -O <sub>8</sub> O <sub>3</sub> -Sn <sub>1</sub> -O <sub>2</sub> O <sub>6</sub> -Sn <sub>2</sub> -O <sub>8</sub>	215	0.00	0.00	0.00	0.02	0.03	Twisting Twisting Wagging
	O <sub>3</sub> -Sn <sub>1</sub> -O <sub>2</sub>	221	0.02	0.02	0.00	0.00	0.04	Twisting
	O <sub>6</sub> -Sn <sub>2</sub> -O <sub>8</sub>	225	0.02	0.02	0.00	0.02	0.06	Wagging
	O <sub>6</sub> -Sn <sub>2</sub> -O <sub>8</sub>	231	0.02	0.02	0.00	0.00	0.04	Wagging
	O <sub>5</sub> -Sn <sub>1</sub> -O <sub>4</sub> O <sub>5</sub> -Sn <sub>4</sub> -O <sub>4</sub>	250	0.02	0.00	0.01	0.01	0.04	Twisting Twisting
	O <sub>3</sub> -Sn <sub>2</sub> -O <sub>1</sub>	265	0.01	0.01	0.00	0.00	0.02	Wagging
	O <sub>5</sub> -Sn <sub>1</sub> -O <sub>4</sub> O <sub>5</sub> -Sn <sub>4</sub> -O <sub>4</sub>	289	0.00	0.00	0.00	0.00	0.01	Wagging Wagging
	Sn <sub>1</sub> -O <sub>4</sub> -Sn <sub>4</sub> Sn <sub>2</sub> -O <sub>4</sub> -Sn <sub>4</sub> Sn <sub>1</sub> -O <sub>5</sub> -Sn <sub>4</sub> Sn <sub>4</sub> -O <sub>5</sub> -Sn <sub>3</sub>	304	0.03	0.00	0.00	0.00	0.03	Wagging
In-plane	Sn <sub>2</sub> -O <sub>8</sub> -Sn <sub>4</sub> O <sub>8</sub> -Sn <sub>4</sub> -O <sub>7</sub>	390	0.00	0.00	0.00	0.00	0.00	Antisymm. stretching Scissoring Scissoring Scissoring Antisymm. stretching Scissoring Rocking
	O <sub>1</sub> -Sn <sub>2</sub> -O <sub>3</sub> O <sub>1</sub> -Sn <sub>2</sub> -O <sub>3</sub> Sn <sub>2</sub> -O <sub>8</sub> -Sn <sub>4</sub> O <sub>8</sub> -Sn <sub>4</sub> -O <sub>7</sub>	414	0.01	0.00	0.00	0.00	0.01	
	O <sub>1</sub> -Sn <sub>2</sub> -O <sub>3</sub> O <sub>1</sub> -Sn <sub>2</sub> -O <sub>3</sub> Sn <sub>2</sub> -O <sub>3</sub> -Sn <sub>1</sub> O <sub>8</sub> -Sn <sub>4</sub> -O <sub>7</sub>	449	0.00	0.00	0.00	0.00	0.00	Symmetrical stretching
	O <sub>1</sub> -Sn <sub>2</sub> -O <sub>3</sub> O <sub>1</sub> -Sn <sub>2</sub> -O <sub>3</sub> Sn <sub>2</sub> -O <sub>8</sub> -Sn <sub>4</sub> O <sub>8</sub> -Sn <sub>4</sub> -O <sub>7</sub> O <sub>1</sub> -Sn <sub>2</sub> -O <sub>6</sub>	456	0.00	0.00	0.00	0.00	0.00	Rocking Rocking Symmetrical stretching Scissoring Scissoring Rocking
	Sn <sub>1</sub> -O <sub>5</sub> -Sn <sub>4</sub>	494	0.00	0.00	0.00	0.00	0.02	
	Sn <sub>4</sub> -O <sub>5</sub> -Sn <sub>3</sub> Sn <sub>1</sub> -O <sub>5</sub> -Sn <sub>4</sub>	508	0.00	0.00	0.00	0.01	0.01	Antisymm. stretching
	C-Sn <sub>2</sub> -C C-Sn <sub>4</sub> -C	517	0.00	0.00	0.00	0.00	0.00	Symmetrical stretching
	C-Sn <sub>2</sub> -C C-Sn <sub>4</sub> -C	519	0.00	0.00	0.00	0.00	0.01	Symmetrical stretching

C-Sn <sub>3</sub> -C	523	0.00	0.00	0.03	0.00	0.03	Symmetrical stretching
Sn <sub>2</sub> -O <sub>8</sub> -Sn <sub>4</sub> O <sub>8</sub> -Sn <sub>4</sub> -O <sub>7</sub>	551	0.00	0.00	0.00	0.00	0.00	Antisymm. stretching Scissoring
C-Sn <sub>3</sub> -C	561	0.00	0.00	0.06	0.00	0.06	Antisymm. stretching
Sn <sub>2</sub> -O <sub>8</sub> -Sn <sub>4</sub> O <sub>8</sub> -Sn <sub>4</sub> -O <sub>7</sub> C-Sn <sub>1</sub> -C O <sub>3</sub> -Sn <sub>1</sub> -O <sub>2</sub>	563	0.01	0.00	0.00	0.00	0.01	Sym.str. Antisymm. Str. Antisymm. Str. Antisymm. Str.
C-Sn <sub>4</sub> -C C-Sn <sub>1</sub> -C O <sub>3</sub> -Sn <sub>1</sub> -O <sub>2</sub> C-Sn <sub>4</sub> -C	570	0.03	0.00	0.00	0.01	0.03	stretching Antisymm. stretching
C-Sn <sub>1</sub> -C O <sub>3</sub> -Sn <sub>1</sub> -O <sub>2</sub> Sn <sub>1</sub> -O <sub>3</sub> -Sn <sub>2</sub>	576	0.00	0.00	0.00	0.06	0.06	Antisymm. stretching
C-Sn <sub>1</sub> -C O <sub>3</sub> -Sn <sub>1</sub> -O <sub>2</sub> Sn <sub>1</sub> -O <sub>3</sub> -Sn <sub>2</sub>	587	0.04	0.00	0.00	0.00	0.04	Antisymm. str. Rocking
C-Sn <sub>1</sub> -C	590	0.03	0.01	0.00	0.00	0.04	Antisymm. stretching
C-Sn <sub>2</sub> -C	592	0.00	0.06	0.00	0.00	0.06	Antisymm. stretching
Sn <sub>1</sub> -O <sub>4</sub> -Sn <sub>4</sub> Sn <sub>2</sub> -O <sub>4</sub> -Sn <sub>4</sub>	637	0.01	0.00	0.00	0.00	0.02	Rocking
Sn <sub>1</sub> -O <sub>5</sub> -Sn <sub>4</sub> Sn <sub>1</sub> -O <sub>4</sub> -Sn <sub>4</sub>	653	0.01	0.00	0.01	0.00	0.02	Rocking
Sn <sub>1</sub> -O <sub>5</sub> -Sn <sub>4</sub> Sn <sub>1</sub> -O <sub>4</sub> -Sn <sub>4</sub>	666	0.01	0.00	0.01	0.00	0.01	Rocking
Sn <sub>1</sub> -O <sub>5</sub> -Sn <sub>4</sub> Sn <sub>1</sub> -O <sub>4</sub> -Sn <sub>4</sub> Sn <sub>1</sub> -O <sub>4</sub> -Sn <sub>2</sub>	738	0.00	0.00	0.00	0.00	0.01	Symmetrical stretching
Cl-Sn <sub>3</sub> -Cl	276	0.00	0.00	0.04	0.00	0.04	Antisymm. stretching

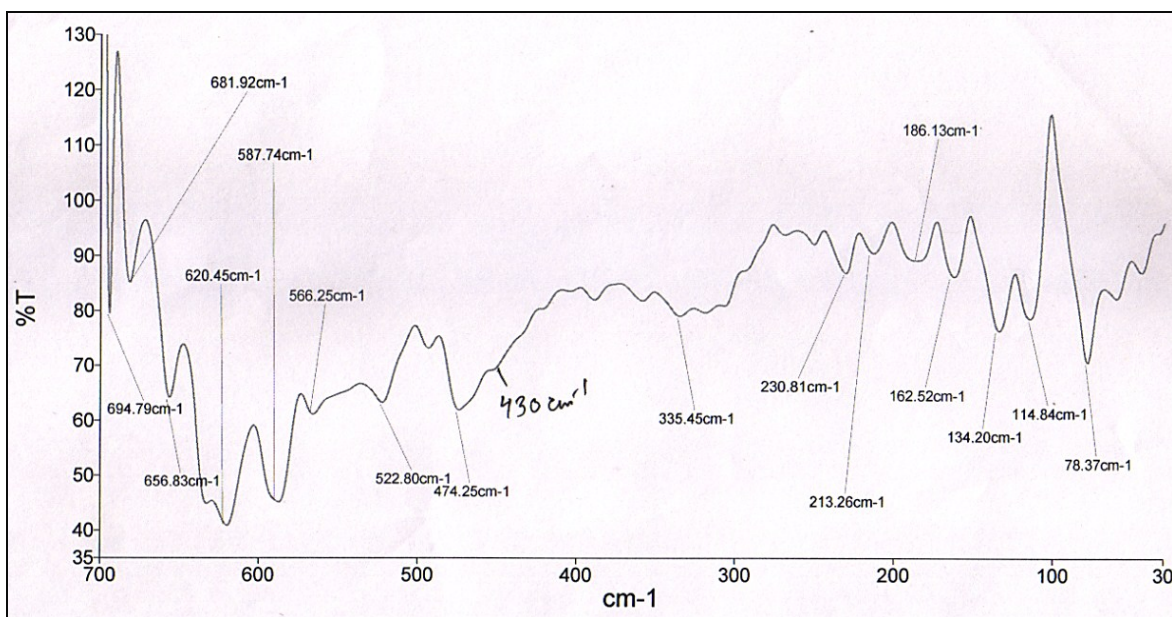


Fig. S1 Far-IR spectrum of 1.

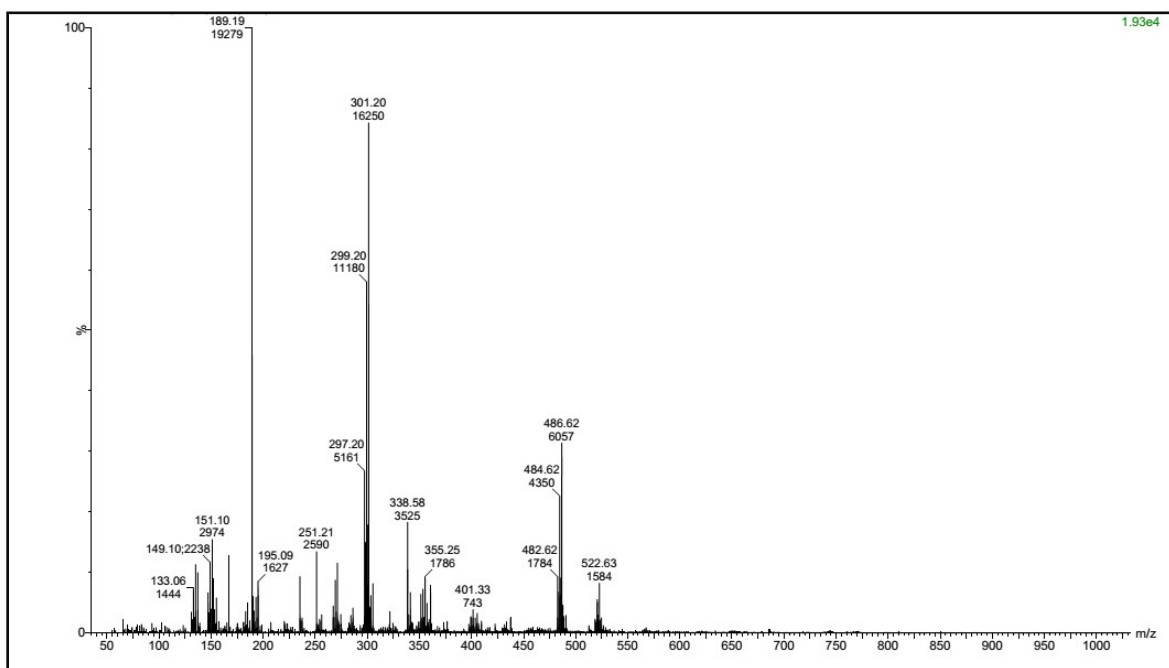
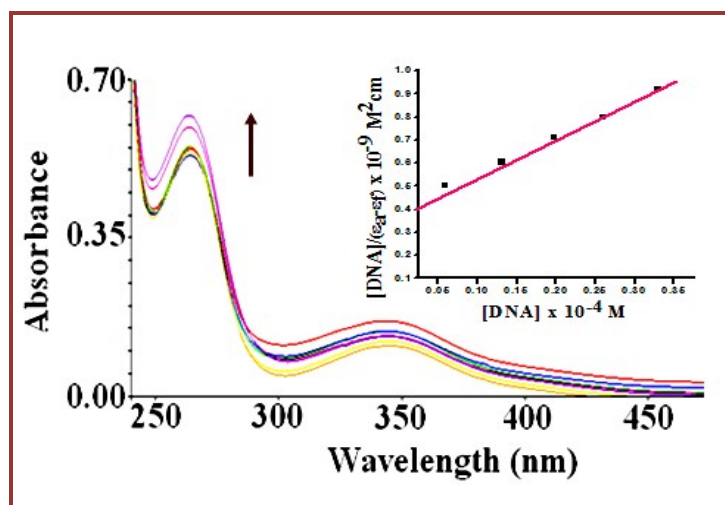
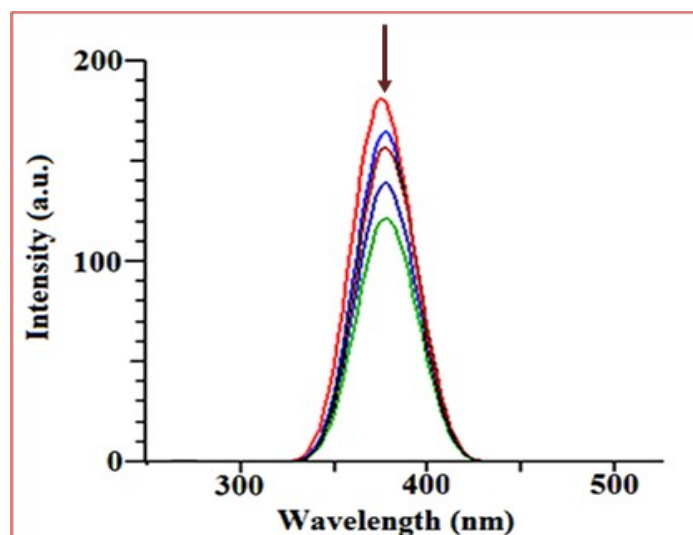


Fig. S2 ESI mass spectrum of 1.



**Fig. S3** UV-vis spectra of **1** in Tris-HCl buffer at pH 7.2 upon addition CT-DNA, [DNA] = 0.00–4.00 × 10<sup>-5</sup> M, [**1**] = 1.0 × 10<sup>-5</sup> M. Arrow indicates change in absorbance with increasing concentration of CT-DNA.

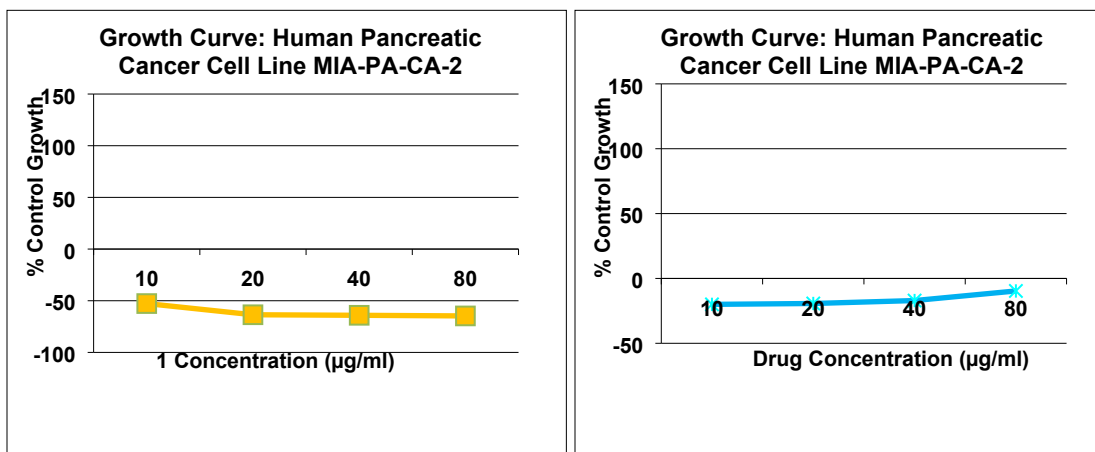


**Fig. S4** Effect of different concentrations of NaCl on emission spectrum of [CT-DNA-complex **1**] system. Arrow indicates the gradual decrease in emission intensity as a function of NaCl concentration.

### ***In vitro* antitumor activity**

The human cancer cell lines of different histological origin, used *in vitro* antitumor screening of **1** were following *viz.*, MCF-7 (breast), MIA-PA-CA-2 (pancreatic), HeLa (Cervix), and Hep-G2 (Hepatoma). Human malignant cell lines were procured and grown in RPMI-1640 medium supplemented with 10% Fetal Bovine Serum (FBS) and antibiotics to study growth pattern of

these cells. The proliferation of the cells upon treatment with chemotherapy was determined by means of the SRB semi-automated assay. All cell lines were seeded into 96 well plates and cells were counted and cell count was adjusted according to the titration readings so as to give optical density in the linear range (0.5 to 1.8) and were incubated at 37 °C in CO<sub>2</sub> incubator for 24 h. The stock solution of the complexes were prepared as 100 mg/ml in DMSO and four dilutions i.e. 10 µg/ml, 20 µg/ml, 40 µg/ml, 80 µg/ml, in triplicates were tested, each well receiving 90 µL of cell suspension. The plates were labeled properly and were incubated for 48 h. Termination of experiment was done by gently layering the cells with 50 µL of chilled 30% TCA (in case of adherent cells) and 50% TCA (in case of suspension cell lines) for cell fixation and kept at 4 °C for 1h. Plates stained with 50 µL of 0.4% SRB for 20 min. Fig. S5 depicts the antitumor screening data which shows % control growth vs. drug concentration (µgml<sup>-1</sup>) against four human cancer cell lines.



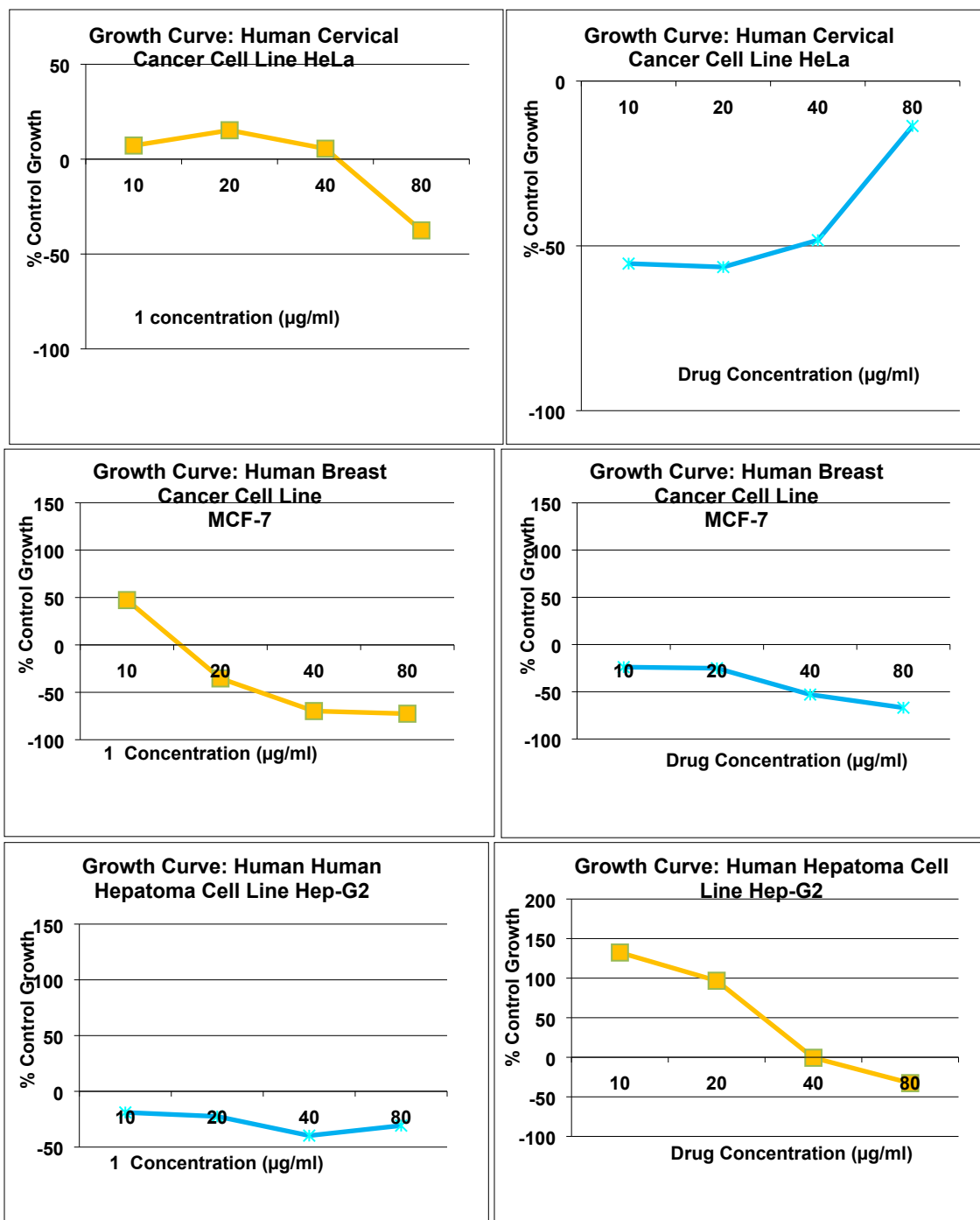


**Fig. S5** Growth curve showing % control vs. drug or complex concentration (µg/ml) against three human cancer cell lines MIA-PA-CA-2 (pancreatic), HeLa (cervical), MCF-7 (breast) and Hep-G2 (Hepatoma).



**Table S6.** Selected bond angles [deg] of complex **1**

<b>Bond Angle</b>	<b>Experimental</b>	<b>Calculated</b>
O(4)-Sn(1)-O(5)	74.16(17)	73.94
O(4)-Sn(1)-O(3)	68.90(14)	64.00
O(5)-Sn(1)-O(3)	142.89(14)	146.61
O(4)-Sn(2)-O(3)#1	69.98(9)	65.91
O(4)-Sn(2)-O(3)	69.98(9)	73.03
O(1)-Sn(2)-O(1)#1	72.29(18)	74.26
O(5)-Sn(3)-Cl(1)	83.48(3)	87.84
O(5)-Sn(3)-Cl(1)#1	83.48(3)	78.96
C(2)-Sn(3)-Cl(1)#1	92.50(5)	96.16
C(1)-Sn(3)-Cl(1)#1	92.62(4)	88.27
Cl(1)-Sn(3)-Cl(1)#1	166.96(7)	166.79
Sn(2)-O(3)-Sn(1)	96.13(13)	96.10
Sn(1)-O(4)-Sn(1)#1	110.4(2)	108.71
Sn(1)-O(4)-Sn(2)	124.72(12)	126.37
Sn(1)#1-O(4)-Sn(2)	124.72(12)	124.92
Sn(3)-O(5)-Sn(1)#1	128.89(11)	125.01
Sn(3)-O(5)-Sn(1)	128.89(11)	132.18
Sn(1)#1-O(5)-Sn(1)	101.1(2)	102.81

**Table S7.** DFT-optimized structure coordinates of complex **1**.

Atom	X	Y	Z
Sn	-0.143307000	2.984990000	7.808475000
Sn	-0.972553000	4.880664000	10.793547000
Sn	0.760644000	4.517874000	4.458167000
Cl	0.688894000	7.169237000	4.926127000
O	-1.467750000	3.316713000	12.576315000
O	-0.258046000	0.381585000	8.369253000
O	-0.702345000	2.454909000	9.955101000
O	-0.425825000	4.731374000	8.809353000
O	0.231903000	4.552356000	6.386922000
C	2.865705000	4.671394000	4.064147000
H	3.060207000	5.477539000	3.343313000
H	3.371325000	4.921375000	5.008183000
C	-0.842416000	4.788154000	3.054676000
H	-0.537405000	5.498888000	2.273665000
H	-1.130858000	3.828333000	2.605355000
C	1.912614000	2.426230000	8.014921000
H	2.251704000	1.931871000	7.094104000
H	2.501106000	3.342370000	8.167248000
H	2.046822000	1.754821000	8.873041000
C	-2.026327000	2.412550000	6.963776000
H	-1.862415000	1.757345000	6.097624000
H	-2.649348000	1.903347000	7.711861000
H	-2.531876000	3.326241000	6.619457000
C	1.012494000	4.753150000	11.565443000
H	1.039317000	4.981786000	12.639803000
H	1.397785000	3.738521000	11.392252000
C	-3.080252000	4.771855000	10.470481000
H	-3.628466000	4.933287000	11.408161000
H	-3.362359000	5.541506000	9.738232000
C	-1.497345000	2.100060000	12.758959000
H	-1.785653000	1.743386000	13.775400000
C	-1.214611000	1.031789000	11.824966000
C	-1.342386000	-0.294824000	12.319277000
H	-1.638064000	-0.432723000	13.362708000
C	-1.118235000	-1.386281000	11.509486000
H	-1.224216000	-2.401989000	11.895470000
C	-0.752416000	-1.180621000	10.161737000
H	-0.569625000	-2.042059000	9.518281000
C	-0.614694000	0.100941000	9.654434000
C	-0.839489000	1.265329000	10.467371000
C	-0.089457000	-0.659008000	7.423786000
H	0.166854000	-0.172085000	6.473322000
H	0.728263000	-1.336698000	7.721689000
H	-1.020824000	-1.239279000	7.306159000
H	3.250928000	3.715166000	3.683947000
H	-1.697672000	5.218295000	3.595863000
H	1.641468000	5.468985000	11.018376000
H	-3.334303000	3.783751000	10.060858000
Sn	-0.068059000	6.293512000	7.523186000

Cl	0.692126000	2.016746000	4.582253000
O	-1.476969000	6.204271000	12.685632000
O	-0.285665000	8.963165000	8.381615000
O	-0.750566000	6.968542000	10.039958000
C	1.911798000	6.868910000	8.099236000
H	2.276899000	7.673844000	7.449609000
H	2.558734000	5.988081000	975660000
H	1.917395000	7.190022000	9.148947000
C	-2.060770000	6.872856000	6.993084000
H	-2.043540000	7.677245000	6.246917000
H	-2.608301000	7.194792000	7.888194000
H	-2.550666000	5.990493000	6.555446000
C	-1.509866000	7.429928000	12.841421000
H	-1.788014000	7.804725000	13.852166000
C	-1.236935000	8.461078000	11.874069000
C	-1.349810000	9.807889000	12.318062000
H	-1.637157000	9.991021000	13.356858000
C	-1.116245000	10.857661000	11.460835000
H	-1.207462000	11.890506000	11.802665000
C	-0.756107000	10.591088000	10.120011000
H	-0.565868000	11.427149000	9.446470000
C	-0.633929000	9.291045000	9.656298000
C	-0.872947000	8.166057000	10.522869000
C	-0.049819000	9.987210000	7.433124000
H	0.214285000	9.483787000	6.493418000
H	0.784634000	10.636940000	7.748185000
H	-0.952770000	10.604138000	7.281922000

## References

1. F. Neese, *Wiley Interdiscip. Rev.: Comput. Mol. Sci.* **2**, 2012, 73-78; F. Neese, "Orca." An ab Initio, *Density Functional and Semiempirical Program Package version 2*, 2009.
2. C. Lee, W. Yang and R. G. Parr, *Phys. Rev. B.; Condens. Matter Mater. Phys.*, 1988, **37**, 785; A. Schaefer, H. Horn and R. Ahlrichs, *J. Chem. Phys.*, 1992, **97**, 2571.
3. F. Weigend and R. Ahlrichs, *Phys. Chem. Chem. Phys.*, 2005, **7**, 3297-3305; A. Schaefer, C. Huber and R. Ahlrichs, *J. Chem. Phys.*, 1994, **100**, 5829; S. Grimme, S. Ehrlich and L. Goerigk, *J. Comput. Chem.*, 2011, **32**, 1456; S. Grimme, J. Antony, S. Ehrlich and H. Krieg, *J. Chem. Phys.*, 2010, **132**, 154104.
4. B. M. Leu, M. Z. Zgierski, C. Bischoff, M. Li, M. Y. Hu, J. Zhao, S. W. Martin, E. E. Alp and W. R. Scheidt, *Inorg. Chem.*, 2013, **52**, 9948.
5. T. S. Toellner, A. Alatas and A. H. Said, *J. Synchrotron Radiat.*, 2011, **18**, 605-611; B. M. Leu, M. Sturza, M. Y. Hu, D. Gosztola, V. Baran, T. F. Fassler and E. E. Alp, *Phys. Rev. B.*, 2014, **90**, 104304.

6. W. Sturhahn, *Hyperfine Interactions*, 2000, **125**, 149.
7. F. Arjmand and M. Muddassir, *Chirality*, 2011, **23**, 250–259; I. Yousuf, F. Arjmand, S. Tabassum, L. Toupet, R. A. Khan and M. A. Siddiqui, *Dalton Trans.*, 2015, **44**, 10330–10342.
8. J. R. Lakowicz and G. Webber, *Biochemistry*, 1973, **12**, 4161.
9. F. Arjmand, I. Yousuf, M. Afzal and L. Toupet, *Inorg. Chim. Acta*, 2014, **421**, 26–37; M. Chauhan, K. Banerjee and F. Arjmand, *Inorg. Chem.*, 2007, **46**, 3072.
10. D. Mustard and D. W. Ritchie, *Proteins: Struct. Funct. Bioinf.*, 2005, **60**, 269–274; G. Macindoe, L. Mavridis, V. Venkatraman, M.–D. Devignes and D. W. Ritchie, *Nucl. Acids Res.*, 2010, **38**, 445.
11. A. Altomare, M. C. Burla, M. Camalli, G. L. Cascarano, C. Giacavazzo, A. Guagliardi, A. G. C. Moliterni, G. Polidori and S. Spagna, *J. Appl. Crystallogr.*, 1999, **32**, 115.
12. G. M. Sheldrick, SHELX–97, *Program for Crystal Structure refinement*, University of Göttingen, Germany, 1997.
13. A. L. Spek, PLATON Procedure, *A multipurpose Crystallographic Tool*, Utrecht University, Utrecht, The Netherlands, 1998.